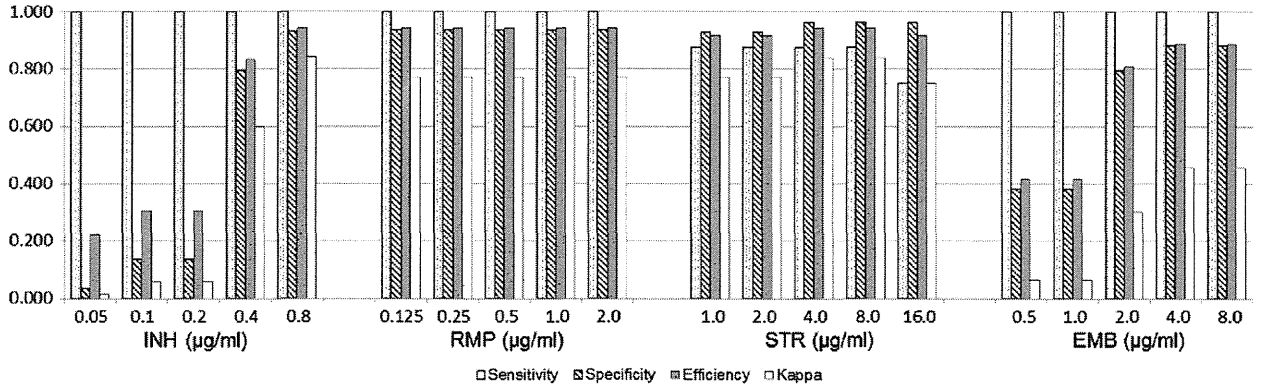

Fig. 3. Performance of MODS compared with the L–J proportion method as a reference by employing the clinical specimen ($n = 36$). Abbreviations: INH, isoniazid; RMP, rifampicin; STR, streptomycin; EMB, ethambutol; Kappa, kappa coefficient; MODS, microscopic observation of drug-susceptibility assay; L–J proportion method, Löwenstein–Jensen proportion method.

sample taken from Japanese also assumes a single mutation of the *rpoB* gene.

The STR concentrations of 4.0 μg/ml or 8.0 μg/ml were the cut-off values with the best combinations of sensitivity and specificity, and the lower concentration of 4.0 μg/ml was determined as the optimal cut-off value for MODS. In previous reports, with reference to the 7H12 liquid culture medium, the critical concentrations of 4.0 μg/ml, 2.0 μg/ml or 6.0 μg/ml were employed as the cut-off values for MODS (Mengatto et al., 2006; Moore et al., 2004, 2006; Park et al., 2002). From the wide concentrations tested in our study, 4.0 μg/ml demonstrated the best discrimination power as the optimal cut-off value between the resistant and the susceptible.

Both 4.0 μg/ml or 8.0 μg/ml of EMB were identified as appropriate cut-off values for MODS with the 36 clinical specimens. The reason for the unsatisfactory Kappa coefficient was that the L–J proportion method showed only 2 EMB-resistant isolates, whereas MODS detected 6 EMB-resistant isolates at both concentrations. Therefore, the misclassification of a small proportion of reference resistant strains affected the Kappa coefficient. This misclassification is rooted in the distinctive feature of the direct (MODS) and the indirect (L–J proportion method) test, and mycobacterial subpopulations of the low-level and the high-level resistance to EMB (Alcaide et al., 1997). One of the advantages of the direct test is that the result represents the patients' original bacterial population and the indirect method alters the proportion of subpopulations resistant to EMB during culture. Therefore, the result of the direct test is more likely to reflect susceptibility to EMB of sputum specimens. Considering those condition, the concentration of 4.0 μg/ml of EMB was the optimal cut-off value for MODS.

The discrimination power of MODS for EMB was particularly poor in comparison with MGIT AST (data not shown). It appeared to be attributed to the unreliability of MGIT AST as a reference. Looking at the efficiency (overall agreement) of DST for EMB using reference strains of known drug susceptibility, the efficiency was 56.8% with MGIT AST compared with 100% with the L–J proportion method. Therefore, MGIT AST was not appropriate for the DST of EMB. Accordingly, Giampaglia et al. (2007) reported that the agreement between MGIT AST and the L–J proportion method for EMB is suboptimal. Piersimoni et al. (2006) mentioned that strains with a low level of resistance are difficult to classify because they are composed of different mycobacterial subpopulations.

Considering the diversity of TB strains, there is a possibility of different MICs among the study strains. The best approach for determination of the optimal cut-off values of MODS is to test a broad range of concentrations based on the diverse study populations, not to transfer the cut-off values from other broth-based drug susceptibility tests.

MODS demonstrated a shorter turnaround time than the L–J proportion method. Most DST results by MODS were obtained within 2 weeks even for the paucibacillary cases and the smear negative cases. In addition, MODS indicated shorter turnaround time than another direct DST method which is recently proposed. The direct inoculation of decontaminated specimens onto an acid-buffered solid medium (direct DST by the Kudoh-modified Ogawa medium) reported to have a shorter turnaround time (>83% of resistant results by 4 weeks) than the indirect DST by the L–J proportion method, and shows reliable results for INH and RMP (Kim et al., 2013). Even though the direct DST by the Kudoh-modified Ogawa medium shortens turnaround time of DST, it will be adopted to sputum smear positive specimens only in general due to high failure rate of DST for scanty smear positive sputum specimens. In terms of rapid diagnosis and applicability to smear negative cases, MODS has an advantage over the direct DST by the Kudoh-modified Ogawa medium. Since there have been only a few articles referring to turnaround time with the direct DST for smear negative TB patients with MODS, our result confirmed the use of smear negative sputa for MODS, and indicated a shorter turnaround time in such specimens (Moore et al., 2004, 2006; Shah et al., 2011). Even though we still primarily need the conventional indirect DST due to occasional no growth in MODS, it will be useful for rapid diagnosis of drug resistant TB, even with a smear negative specimen. The fact will expand the use of MODS in clinical settings.

5. Conclusion

We evaluated the optimal cut-off values for MODS for the four first-line drugs from the broad range of concentrations. With those cut-off values, MODS demonstrated the reliable discrimination powers and short turnaround time even for smear negative cases. MODS is useful in terms of rapid diagnosis of drug resistant TB.

Acknowledgment

This study was supported by a health science research grant of the Ministry of Health, Welfare and Labor (H20-Shinko-Ippan-016).

References

Alcaide, F., Pfyffer, G.E., Telenti, A., 1997. Role of *embB* in natural and acquired resistance to ethambutol in mycobacteria. Antimicrob. Agents Chemother. 41, 2270–2273.

Bwanga, F., Joloba, M.L., Haile, M., et al., 2010. Evaluation of seven tests for the rapid detection of multidrug-resistant tuberculosis in Uganda. Int. J. Tuberc. Lung Dis. 14, 890–895.

Caviedes, L., Lee, T.S., Gilman, R.H., et al., 2000. Rapid, efficient detection and drug susceptibility testing of *Mycobacterium tuberculosis* in sputum by microscopic observation of broth cultures. J. Clin. Microbiol. 38, 1203–1208.

Coronel, J., Roper, H., Caviedes, L., et al., 2008. MODS: A User Guide. Universidad Peruana Cayetano Heredia, Lima, Peru (http://www.modsperu.org/MODS_user_guide.pdf Accessed December 2013).

Dixit, P., Singh, U., Sharma, P., et al., 2012. Evaluation of nitrate reduction assay, resazurin microtiter assay and microscopic observation drug susceptibility assay for first line

antitubercular drug susceptibility testing of clinical isolates of *M. tuberculosis*. J. Microbiol. Methods 88, 122–126.
Giampaglia, C.M.S., Martins, M.C., Vieira, G.B.O., et al., 2007. Multicentre evaluation of an automated BACTEC 960 system for susceptibility testing of *Mycobacterium tuberculosis*. Int. J. Tuberc. Lung Dis. 11, 986–991.
Hardy Diagnostics, a. TB MODS kit for TB identificationhttp://hardydiagnostics.com/tbmodskit.html (Accessed March 2014).
Kim, C.K., Joo, Y.T., Lee, E.P., et al., 2013. Simple, direct drug susceptibility testing technique for diagnosis of drug-resistant tuberculosis in resource-poor settings. Int. J. Tuberc. Lung Dis. 17, 1212–1216.
Limaye, K., Kanade, S., Nataraj, G., et al., 2010. Utility of microscopic observation of drug susceptibility (MODS) assay for *Mycobacterium tuberculosis* in resource constrained settings. Indian J. Tuberc. 57, 207–212.
Makamure, B., Mhaka, J., Makumbirofa, S., et al., 2013. Microscopic-observation drug-susceptibility assay for the diagnosis of drug-resistant tuberculosis in Harare, Zimbabwe. PLoS One 8, e55872.
Mello, F.C.Q., Arias, M.S., Rosales, S., et al., 2007. Clinical evaluation of the microscopic observation drug susceptibility assay for detection of *Mycobacterium tuberculosis* resistance to isoniazid and rifampin. J. Clin. Microbiol. 45, 3387–3389.
Mengatto, L., Chiani, Y., Imaz, M.S., 2006. Evaluation of rapid alternative methods for drug susceptibility testing in clinical isolates of *Mycobacterium tuberculosis*. Mem. Inst. Oswaldo Cruz 101, 535–542.
Minion, J., Leung, E., Menzies, D., et al., 2010. Microscopic-observation drug susceptibility and thin layer agar assays for the detection of drug resistant tuberculosis: a systematic review and meta-analysis. Lancet Infect. Dis. 10, 688–698.
Moore, D.A.J., Mendoza, D., Gilman, R.H., et al., 2004. Microscopic observation drug susceptibility assay, a rapid, reliable diagnostic test for multidrug-resistant tuberculosis suitable for use in resource-poor settings. J. Clin. Microbiol. 42, 4432–4437.
Moore, D.A.J., Evans, C.A.W., Gilman, R.H., et al., 2006. Microscopic-observation drug-susceptibility assay for the diagnosis of TB. N. Engl. J. Med. 355, 1539–1550.
Park, W.G., Bishai, W.R., Chaisson, R.E., et al., 2002. Performance of the microscopic observation drug susceptibility assay in drug susceptibility testing for *Mycobacterium tuberculosis*. J. Clin. Microbiol. 40, 4750–4752.
Piersimoni, C., Armando, O., Benacchio, L., et al., 2006. Current perspectives on drug susceptibility testing of *Mycobacterium tuberculosis* complex: the automated nonradiometric systems. J. Clin. Microbiol. 44, 20–28.
Shah, N.S., Moodley, P., Babaria, P., et al., 2011. Rapid diagnosis of tuberculosis and multidrug resistance by the microscopic-observation drug-susceptibility assay. Am. J. Respir. Crit. Care Med. 183, 1427–1433.
Shiferaw, G., Woldeamanuel, Y., Gebeyehu, M., et al., 2007. Evaluation of microscopic observation drug susceptibility assay for the detection of multidrug-resistant *Mycobacterium tuberculosis*. J. Clin. Microbiol. 45, 1093–1097.
Suzuki, Y., Katsukawa, C., Inoue, K., et al., 1995. Mutations in *rpoB* gene of rifampicin resistant clinical isolates of *Mycobacterium tuberculosis* in Japan. Kansenshogaku Zasshi 69, 413–419.
Telenti, A., Imboden, P., Marchesi, F., et al., 1993. Detection of rifampicin-resistance mutations in *Mycobacterium tuberculosis*. Lancet 341, 647–650.

Chikamatsu et al. BMC Infectious Diseases 2014, 14:54
http://www.biomedcentral.com/1471-2334/14/54

BMC
Infectious Diseases

RESEARCH ARTICLE Open Access

Comparative evaluation of three immunochromatographic identification tests for culture confirmation of *Mycobacterium tuberculosis* complex

Kinuyo Chikamatsu[1*], Akio Aono[1], Hiroyuki Yamada[1], Tetsuhiro Sugamoto[1], Tomoko Kato[1,2], Yuko Kazumi[1], Kiyoko Tamai[3], Hideji Yanagisawa[3] and Satoshi Mitarai[1,2]

Abstract

Background: The rapid identification of acid-fast bacilli recovered from patient specimens as *Mycobacterium tuberculosis* complex (MTC) is critically important for accurate diagnosis and treatment. A thin-layer immunochromatographic (TLC) assay using anti-MPB64 or anti-MPT64 monoclonal antibodies was developed to discriminate between MTC and non-tuberculosis mycobacteria (NTM). Capilia TB-Neo, which is the improved version of Capilia TB, is recently developed and needs to be evaluated.

Methods: Capilia TB-Neo was evaluated by using reference strains including 96 *Mycobacterium* species (4 MTC and 92 NTM) and 3 other bacterial genera, and clinical isolates (500 MTC and 90 NTM isolates). *M. tuberculosis* isolates tested negative by Capilia TB-Neo were sequenced for *mpt64* gene.

Results: Capilia TB-Neo showed 100% agreement to a subset of reference strains. Non-specific reaction to *M. marinum* was not observed. The sensitivity and specificity of Capilia TB-Neo to the clinical isolates were 99.4% (99.6% for *M. tuberculosis,* excluding *M. bovis* BCG) for clinical MTC isolates and 100% for NTM isolates tested, respectively. Two *M. tuberculosis* isolates tested negative by Capilia TB-Neo: one harbored a 63-bp deletion in the *mpt64* gene and the other possessed a 3,659-bp deletion from Rv1977 to Rv1981c, a region including the entire *mpt64* gene.

Conclusions: Capilia TB-Neo is a simple, rapid and highly sensitive test for identifying MTC, and showed better specificity than Capilia TB. However, Capilia TB-Neo still showed false-negative results with *mpt64* mutations. The limitation should be recognized for clinical use.

Keywords: Capilia TB-Neo, *Mycobacterium tuberculosis* complex identification, *mpt64* gene

Background

Tuberculosis remains a major threat to global health, and therefore, rapid identification of the causative *M. tuberculosis* complex (MTC) is critical. Liquid culture detection is now widely used for managing HIV-co-infected and drug-resistant tuberculosis, and liquid culture can improve the recovery of acid-fast bacilli and decreases the time to detection. However, because other non-tuberculosis mycobacterium (NTM) species may also grow, it is important to identify MTC from positive culture for rapid and appropriate management of tuberculosis.

Several methods are available to identify mycobacteria. Conventional biochemical tests are generally time-consuming [1,2] and not surely reproducible, while more recently developed techniques involving molecular biology [3-7] or high-performance liquid chromatographic analysis of mycolic acid [8] are accurate and rapid, but these require expensive devices. In contrast, immunochromatographic species identification tests, Capilia TB (TAUNS,

* Correspondence: chikamatsu@jata.or.jp
[1]Department of Mycobacterium Reference and Research, Research Institute of Tuberculosis, Japan Anti-Tuberculosis Association, Kiyose, Tokyo 204-8533, Japan
Full list of author information is available at the end of the article

Izunokuni, Japan), SD BIOLINE TB Ag MPT64 rapid (Standard Diagnostics, Inc., Korea) and BD MGIT™ TBc Identification Test (Becton, Dickinson and Company, USA) have been adopted as a cheap, rapid, and accurate alternative in clinical laboratories around the world [9-11]. However, false positives to *Mycobacterium marinum*, *Staphylococcus aureus* [9,12], and false negatives in MPB64 mutants [10,13] have occasionally been reported. Capilia TB-Neo (TAUNS, Izunokuni, Japan), an improved version of Capilia TB, has recently been developed to overcome these problems. In this study, we evaluated the performance of Capilia TB-Neo with reference strains and clinical isolates. Any false-negative MTC clinical isolate detected by Capilia TB-Neo were further investigated relative genes.

Methods

Reference strains and clinical isolates

Reference strains of 96 *Mycobacterium* species and subspecies (4 MTC and 92 NTM) and 3 other genera with acid-fastness (*Nocardia asteroids*, *Rhodococcus equi* and *Rhodococcus aichiense*) were used for the evaluation (Table 1). A total of 500 MTC and 90 NTM clinical isolates (10 *M. abscessus*, 4 *M. chelonae*, 13 *M. fortuitum*, 8 *M. gordonae*, 15 *M. avium* complex, 7 *M. intracellulare*, 3 *M. nonchromogenicum*, 5 *M. scrofulaceum*, 4 *M. xenopi*, 15 *M. kansasii*, 1 *M. gastri*, 2 *M. peregrinum*, 1 *M. intermedium*, 1 *M. szulgai*, and 1 *M. marinum*) were selected to provide a representative sample of the isolates available from Miroku Medical Laboratory Co., Ltd. (Saku, Japan) from 2009 to 2010, and the collection from the Ryoken survey in 2002 and 2007. The clinical isolates were collected from patients as a part of routine examination. No ethical approval was required for this type of laboratory based study only using isolates. Reference strains and clinical isolates were cultured with OADC-supplemented Middlebrook 7H9 broth (Becton, Dickinson and Company, USA) and 2% Ogawa medium (Kyokuto Pharmaceutical Industrial Co., Japan) at 37°C or 30°C.

Identification of mycobacteria

Mycobacterium species of the clinical isolates were identified using one or more of the following approaches: (i) the DNA or RNA amplification kits Cobas Amplicor PCR (Roche Diagnostics, Japan) and TRC Rapid (Tosoh Bioscience, Japan); (ii) the DNA-DNA hybridization DDH Mycobacteria Kit (Kyokuto Pharmaceutical Industrial Co., Japan); and (iii) 16S rRNA gene sequencing, supplementary [7]. The isolates identified as MTC were further examined by multiplex PCR analysis of *cfp32*, the region of difference (RD) 9, and RD12 according to the method of Nakajima et al. [14]. When MTC species other than *M. tuberculosis* sensu stricto were detected, they were further characterized with respect to RD1, RD4, RD7, and MiD3 [15]. If *M. bovis* Bacillus Calmette-Guerin (BCG) was identified, additional multiplex PCR analyses were performed to test for RD2, RD14, RD15, RD16, and *SenX3-RegX3* to distinguish sub-strains of BCG [16,17]. The multiplex PCR amplification was performed using a Type-it Microsatellite PCR Kit (QIAGEN, Japan). Each PCR reaction contained 1.0 μl of DNA template, 6.25 μl of Type-it multiplex PCR Master mix, 1.25 μl of Q-solution, 0.25 μl of each primer (10 pmol/μl) and an appropriate amount of molecular grade water for a total reaction volume of 13 μl. The thermal profile was as follows: (i) 95°C (5 min); (ii) 28 cycles of 95°C (0.5 min), 58 or 55°C (1.5 min), 72°C (0.5 min); and (iii) a final extension step at 68 or 60°C (10 or 30 min). The amplified products were analyzed by 3% agarose gel electrophoresis. The expected RD loci for each MTC species are summarized in Table 2.

Capilia TB-Neo, SD MPT64, and TBc ID

The validation of Capilia TB-Neo (TAUNS, Izunokuni, Japan) was conducted using the aforementioned reference strains as well as MTC and NTM clinical isolates. In addition, SD BIOLINE TB Ag MPT64 rapid (SD MPT64: Standard Diagnostics, Inc. Korea) and BD MGIT™ TBc Identification Test (TBc ID: Becton, Dickinson and Company, USA), detect MPT64 which is the same as MPB64, were tested using reference strains and NTM clinical isolates. Each test was performed according to the manufacturer's instructions. Briefly, clinical isolates growing on Ogawa medium were suspended in 1 ml of sterile distilled water, and the suspension subjected to the test. Similarly, positive liquid cultures of reference strains (McFarland No. 1 to 2) were directly subjected to each test. Positive test results were indicated by a red line in the test area after 15 min.

Sequencing of the *mpt64* gene

Any false-negative *M. tuberculosis* isolate detected by Capilia TB-Neo was further analyzed by sequencing *mpt64* and surrounding genes by using the primers listed in Table 2. Each PCR reaction contained 1.0 μl of DNA template, 12.5 μl of Type-it multiplex PCR Master mix, 2.5 μl of Q-solution, 0.5 μl of each primer (10 pmol/μl) and an appropriate amount of molecular grade water for a total reaction volume of 25 μl. The thermal profile was as follows: (i) 95°C (5 min); (ii) 30 cycles of 95°C (0.5 min), 62°C (1.5 min), 72°C (1 min); and (iii) final extension at 60°C (10 min). The amplified product was analyzed by 3% agarose gel electrophoresis and was purified using Mag Extractor (TOYOBO, Japan). The purified DNA products were subjected to direct sequencing using an ABI 377 automatic sequencer (Applied Biosystems, USA) and BigDye Terminator Cycle Sequencing v 3.1 (Applied Biosystems, USA), according to the manufacturer's instructions. DNA

Table 1 List of reference strains and the results of identification of MTC by using Capilia TB-Neo, SD MPT64, and TBc ID

Species	Strain	Capilia TB-Neo	SD MPT64	TBc ID	Species	Strain	Capilia TB-Neo	SD MPT64	TBc ID
M. tuberculosis H37Rv	ATCC27294	+	+	+	*M. interjectum*	ATCC51457	-	-	-
M. africanum	ATCC25420	+	+	+	*M. intermedium*	ATCC51848	-	-	-
M. bovis	ATCC19210	+	+	+	*M. intracellulare*	ATCC13950	-	-	-
M. microti	ATCC19422	+	+	+	*M. kansasii*	ATCC12478	-	-	-
M. abscessus	ATCC19977	-	-	-	*M. kubicae*	ATCC700732	-	-	-
M. acapulcensis	ATCC14473	-	-	-	*M. lactis*	ATCC27356	-	-	-
M. agri	ATCC27406	-	-	-	*M. lentiflavum*	ATCC51985	-	-	-
M. aichiense	ATCC27280	-	-	+	*M. madagascariense*	ATCC49865	-	-	-
M. alvei	ATCC51304	-	-	-	*M. malmoense*	ATCC29571	-	-	-
M. asiaticum	ATCC25276	-	-	-	*M. marinum*	ATCC00927	-	-	+
M. aurum	ATCC23366	-	-	-	*M. moriokaense*	ATCC43059	-	-	-
M. austroafricanum	ATCC33464	-	-	-	*M. mucogenicum*	ATCC49650	-	-	-
M. avium subsp. *avium*	ATCC25291	-	-	-	*M. neoaurum*	ATCC25795	-	-	-
M. avium subsp. *paratuberculosis*	ATCC19698	-	-	-	*M. nonchromogenicum*	ATCC19530	-	-	-
M. avium subsp. *"suis"*	ATCC19978	-	-	-	*M. novum*	ATCC19619	-	-	-
M. avium subsp. *silvaticum*	ATCC49884	-	-	-	*M. obuense*	ATCC27023	-	-	-
M. branderi	ATCC51789	-	-	-	*M. paraffinicum*	ATCC12670	-	-	-
M. brumae	ATCC51384	-	+	-	*M. parafortuitum*	ATCC19686	-	-	-
M. celatum	ATCC51131	-	-	-	*M. peregrinum*	ATCC14467	-	-	-
M. celatum II	ATCC51130	-	-	-	*M. petroleophilum*	ATCC21497	-	-	-
M. chelonae chemovar niacinogenes	ATCC35750	-	-	-	*M. phlei*	ATCC11758	-	-	-
M. chelonae subsp. *chelonae*	ATCC35752	-	-	-	*M. porcinum*	ATCC33776	-	-	-
M. chitae	ATCC19627	-	-	+	*M. poriferae*	ATCC35087	-	-	-
M. chlorophenolicum	ATCC49826	-	-	-	*M. pulveris*	ATCC35154	-	-	-
M. chubuense	ATCC27278	-	-	-	*M. rhodesiae*	ATCC27024	-	-	-
M. confluentis	ATCC49920	-	-	-	*M. scrofulaceum*	ATCC19981	-	-	-
M. conspicuum	ATCC700090	-	-	-	*M. senegalense*	ATCC35796	-	-	-
M. cookii	ATCC49103	-	-	-	*M. septicum*	ATCC700731	-	-	-
M. diernhoferi	ATCC19340	-	-	-	*M. shimoidei*	ATCC27962	-	-	-
M. duvalii	ATCC43910	-	-	-	*M. shinshuense*	ATCC33728	-	-	-
M. engbaekii	ATCC27353	-	-	-	*M. simiae*	ATCC25275	-	-	-
M. flavescens	ATCC14474	-	-	-	*M. smegmatis*	ATCC19420	-	-	-
M. fortuitum subsp. *acetamidolyticum*	ATCC35931	-	-	-	*M. smegmatis*	ATCC700084	-	-	-
M. fortuitum subsp. *fortuitum*	ATCC06841	-	-	-	*M. sphagni*	ATCC33027	-	-	-
M. fortuitum subsp. *fortuitum*	ATCC49403	-	-	-	*M. szulgai*	ATCC35799	-	-	-
M. gadium	ATCC27726	-	-	+	*M. terrae*	ATCC15755	-	-	-
M. gallinarum	ATCC19710	-	-	-	*M. terrae*	DSMZ43540	-	-	-
M. genavense	ATCC51234	-	-	-	*M. terrae*	DSMZ43541	-	-	-
M. gilvum	ATCC43909	-	-	-	*M. terrae*	DSMZ43542	-	-	-
M. goodii	ATCC700504	-	-	-	*M. thermoresistibile*	ATCC19527	-	-	-
M. gordonae	ATCC14470	-	-	-	*M. tokaiense*	ATCC27282	-	-	-
M. gordonae group B[19]	KK33-08	-	-	-	*M. triplex*	ATCC700071	-	-	-
M. gordonae group C[19]	KK33-53	-	-	-	*M. triviale*	ATCC23292	-	-	-

Table 1 List of reference strains and the results of identification of MTC by using Capilia TB-Neo, SD MPT64, and TBc ID *(Continued)*

M. gordonae group D[19]	KK33-46	-	-	-	*M. vaccae*	ATCC15483	-	-	-
M. haemophilum	ATCC29548	-	-	-	*M. valentiae*	ATCC29356	-	-	-
M. hassiacum	ATCC700660	-	-	-	*M. wolinskyi*	ATCC700010	-	-	-
M. heckeshornense	DSMZ44428	-	-	-	*M. xenopi*	ATCC19250	-	-	-
M. heidelbergense	ATCC51253	-	-	-	*Nocardia asteroides*	ATCC19247	-	-	-
M. hiberniae	ATCC49874	-	-	-	*Rhodococcus equi*	ATCC6939	-	-	-
					Rhodococcus aichiense	ATCC33611	-	-	-

sequences of *mpt64* from each isolate were compared with *M. tuberculosis* H37Rv by using Genetyx-win ver. 5.2 (Genetyx Co., Japan).

Results

Each of the three kits (Capilia TB-Neo, SD MPT64, and TBc ID) was tested using the 99 reference strains. Capilia TB-Neo correctly produced positive results for four MTC (*M. tuberculosis*, *M. africanum*, *M. bovis*, and *M. microti*) and negative results for 92 NTM and 3 non-mycobacterial species (other genera) with acid-fastness, while SD MPT64 and TBc ID generated several false positives (Table 1). The sensitivity and specificity of Capilia TB-Neo to reference strains were 100%.

Of the 500 MTC clinical isolates tested, 497 were identified as MTC by Capilia TB-Neo. The other 3 isolates that tested negative by using Capilia TB-Neo also tested negative by using SD MPT64 and TBc ID. All three kits produced negative results for all 90 NTM clinical isolates examined. Thus, The sensitivity and specificity of Capilia TB-Neo to the clinical isolates were 99.4% and 100%, respectively.

The multiplex PCR system identified 492 *M. tuberculosis* isolates out of 500. Five isolates, which were *cfp32*-, RD9-, RD4-, RD7-, and MiD3-positive, but RD12-negative, were initially identified as *M. canettii*. However, colonies of these isolates showed a consistent rough surface on solid medium, and subsequent sequencing of *hsp65* indicated that the isolates had the genotype of *M. tuberculosis* sensu stricto (data not shown). These isolates were collected from different areas of Japan. Consequently, 497 isolates were identified as *M. tuberculosis*. The remaining 3 isolates were deficient in RD1, RD4, RD7, RD9, and RD12, and therefore were identified as *M. bovis* BCG. Two of these isolates were confirmed as *M. bovis* BCG Tokyo based on the unique size of RD16, and the third isolate had the same RD pattern as BCG Connaught and BCG Montreal, as for RD2, RD14, RD15, RD16 and *SenX3-RegX3* (Figure 1). Among the 3 MTC isolates that tested negative by Capilia TB-Neo, 2 isolates were *M. tuberculosis* and the other was *M. bovis* BCG Connaught or BCG Montreal (Table 3).

Mutations in the *mpt64* gene were detected by sequencing two *M. tuberculosis* isolates with negative results by Capilia TB-Neo. One isolate had a deletion of 63 bp from nucleotides 196 to 258 (amino acids position 43 to 63), and the other had a deletion of 3,659 bp from nucleotide 874 in Rv1977 to nucleotide 905 in Rv1981c, which included the whole *mpt64* gene.

Discussion

In many industrialized countries, the ability to rapidly distinguish between MTC and NTM is critical in clinical practice. Indeed, the anti-tuberculosis drug resistance survey in Japan revealed that 19.3% of all clinical mycobacterial isolates are NTM [18], underscoring the importance of rapid and accurate detection of MTC from acid-fast bacillus-positive culture. The immunochromatographic assay kit for the identification of MTC is now widely used in many countries. Capilia TB-Neo is the improved version of Capilia TB, and has been subjected to few clinical evaluations. Here, we report good overall performance of the kit but with several limitations.

In this study, the sensitivity of Capilia TB-Neo was 99.4% to clinical MTC isolates or 99.6% excluding *M. bovis* BCG, while the specificity of the kit tested to clinical NTM isolates was 100%. However, the isolation of BCG could present a practical problem. The *M. bovis* BCG Tokyo strain is sporadically isolated in Japan as a complex of vaccination or bladder cancer therapy, and is identified as MTC with the kit [19]. Some BCG strains such as Connaught, Pasteur, and Tice lack RD2 including the *mpt64* gene, but RD2 is conserved in others such as Tokyo, Moreau, and Russia [16]. This issue should be properly addressed to avoid confusion. Although it is difficult to discriminate BCG Tokyo from MTC with *mpt64*/*mpb64*, their differentiation would be an important advance in the development of a future TLC product. The weak false-positive reaction to *M. marinum* that was reported using Capilia TB [12] was not observed in this study, and resulted in better specificity. The minimum

Table 2 Oligonucleotide primers used in PCR and direct sequencing

Target gene	Primer ID	Nucleotide sequence (5'-3')	Size (bp)	Ref. no.
MTC identification				
16S rRNA	285	GAGAGTTTGATCCTGGCTCAG	1028	7
	264	TGCACACAGGCCACAAGGGA		
	259	TTTCACGAACAACG GACAA	591	
cfp32	Rv0577F	ATGCCCAAGAGAAGCGAATACAGGCAA	786	14
	Rv0577R	CTATTGCTGCGGTGCGGGCTTCAA		
RD9	Rv2073cF	TCGCCGCTGCCAGATGAGTC	600	14
	Rv2073cR	TTTGGGAGCCGCCGGTGGTGATGA		
RD12	Rv3120F	GTCGGCGATAGACCATGAGTCCGTCTCCAT	404	14
	Rv3120R	GCGAAAAGTGGGCGGATGCCAG		
RD1	ET1	AAGCGGTTGCCGCCGACCGACC		15
	ET2	CTGGCTATATTCCTGGGCCCGG		
	ET3	GAGGCGATCTGGCGGTTTGGGG		
RD4	Rv1510F	GTGCGCTCCACCCAAATAGTTGC	1033	15
	Rv1510R	TGTCGACCTGGGGCACAAATCAGTC		
RD7	Rv1970F	GCGCAGCTGCCGGATGTCAAC	1116	15
	Rv1970R	CGCCGGCAGCCTCACGAAATG		
MiD3	IS1561F	GCTGGGTGGGCCCTGGAATACGTGAACTCT	530	15
	IS1561R	AACTGCTCACCCTGGCCACCACCATGGACT		
Distinguish sub-strains of BCG				
RD2	RD2l	CCAGATTCAAATGTCCGACC		16
	RD2r	GTGTCATAGGTGATTGGCTT		
RD14	RD14l	CAGGGTTGAAGGAATGCGTGTC		16
	RD14r	CTGGTACACCTGGGGAATCTGG		
RD15	RD8l	ACTCCTAGCTTTGCTGTGCGCT		16
	RD8r	GTACTGCGGGATTTGCAGGTTC		
RD16	RD16nf	ACATTGGGAAATCGCTGCTGTTG		17
	RD16nr	GGCTGGTGTTTCGTCACTTC		
SenX3-RegX3	C3	GCGCGAGAGCCCGAACTGC		16
	C5	GCGCAGCAGAAACGTCAGC		
Sequencing				
mpt64 (Rv1980c)	mpb64W-F	ACTCAGATATCGCGGCAATC	1061	this study
	mpb64W-R	CGATCACCTCACCTGGAGTT		
Rv1977	Rv1977F	GTTTCCCGAGATCAGCTCAA	348	this study
	Rv1977R	ATCTCGTCGTGTGTCACCAG		
Rv1981c	Rv1981F	GATCGAATGCAGGCTGGTAT	399	this study
	Rv1981R	ACTACTACCGCGGTGACGAC		

detection concentration of *M. tuberculosis* for Capilia TB-Neo was 10^5 CFU/ml (data not shown), which was one-tenth than that for the previous kit. There was a report that Cpilia TB-Neo was higher sensitivity than Capilia TB [20]. In summary, the overall performance of Capilia TB-Neo was better than Capilia TB in both sensitivity and specificity.

SD MPT64 and TBc ID were also tested with reference strains. Both SD MPT64 and TBc ID showed false-positive results against several NTM strains in this study. Kodama et al. [12] reported that no *M. marinum* strains grown on 2% Ogawa medium tested positive by using the Capilia TB, while all strains grown on 3 kinds of liquid medium, MGIT (Becton Dickinson, Japan), KRD

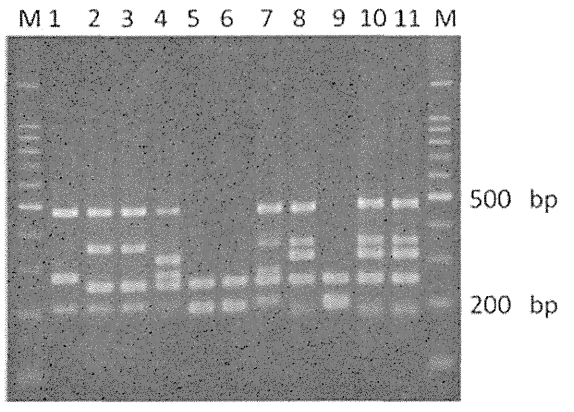

Figure 1 Multiplex PCR analysis of *Mycobacterium bovis* BCG sub-strains and clinical isolates. 1: BCG Pasteur (ATCC35734), 2: BCG Glaxo (ATCC35741), 3: BCG Copenhagen (ATCC27290), 4: BCG Russian (ATCC35740), 5: BCG Montreal (ATCC35735), 6: BCG Connaught (ATCC35745), 7: BCG Danish, 8: BCG Tokyo, 9: Sample 421, 10: Sample 467, 11: Sample 475, M: Size marker.

medium (Japan BCG Laboratory, Japan) and Myco Acid (Kyokuto Pharmaceutical Industrial Co. Ltd., Japan), eventually displayed a positive reaction that intensified with time. Kodama et al. speculated that nonspecific antigen which could make complex with anti-MPB64 antibody may be produced in liquid mediums, but not on solid medium. Considering the effect of liquid culture, the original bacterial suspensions giving false-positive results, that were prepared from liquid and solid culture, were then re-tested before and after 10-fold dilution. Interestingly, none of these diluted strains tested positive in these kits, but bacterial concentrations were high enough for positive results in case of MTC. These results implied that a high concentration of bacterial antigens could induce non-specific reactions in SD MPT64 and TBc ID. The manufacturer's instructions for the TBc ID indicate that this kit may be used up to 10 days after a positive MGIT alarm. This non-specific reaction should be properly addressed in clinical practice, and the users should perform morphological characterization with a microscope to identify cord formation.

Several mutations in the *mpt64* gene produce a negative test result for *M. tuberculosis* isolates in the TLC assay using anti-MPB64 monoclonal antibodies. To date, these include a 63-bp deletion from nucleotide 196, a 1-bp deletion from nucleotide 266, a point mutation at position 388 or 402, *IS6110* insertion mutation at position 177 or 501, a 176-bp deletion from nucleotide 512, and a 1-bp insertion at position 287 [10,13,21]. In our study, 2 *M. tuberculosis* isolates gave false-negative results by using the Capilia TB-Neo, SD MPT64, and TBc ID. One isolate had a deletion of 63 bp from nucleotide 196 in the *mpt64* gene as reported previously, and the other isolate possessed a 3,659-bp deletion from nucleotide 874 in Rv1977 to 905 in Rv1981c, including the whole *mpt64* gene. To the best of our knowledge, this is the first report of a large deletion in *mpt64*. A transposon site hybridization (TraSH) study [22] indicated that *mpt64* is not essential for infection or *in vitro* growth of *M. tuberculosis*. This large deletion mutant supported the finding.

In summary, the TLC assay detecting MPB64 or MPT64 can be applied to specimens prepared from liquid and solid culture. It does not need special reagents, instruments, or complex techniques. Capilia TB-Neo tested in this study showed excellent sensitivity with perfect specificity.

Conclusions

Capilia TB-Neo showed high sensitivity and specificity with clinical mycobacterial isolates, and 100% specificity to reference strains. However, 2 *M. tuberculosis* isolates were tested negative by Capilia TB-Neo because of mutations in the *mpt64* gene, and positive to certain BCG sub-strain. This study, therefore, serves to emphasize the importance of careful use of the kit and the complementary techniques such as morphological identification.

Table 3 Results of PCR detection and Capilia TB-Neo of MTC with clinical isolates

Species interpretation (Number of isolates)	Banding pattern							Capilia TB-Neo	%
	cfp32	RD9	RD12	RD4	RD7	MiD3	RD1		
M. tuberculosis (490)	+	+	+	NT	NT	NT	NT	+	98.0
M. tuberculosis (2)	+	+	+	NT	NT	NT	NT	-	0.4
"M. canettii" (5)[a]	+	+	-	+	+	+	+	+	1.0
M. bovis BCG Tokyo (2)[b]	+	-	-	-	-	+	-	+	0.4
M. bovis BCG Connaught (1)[c]	+	-	-	-	-	+	-	-	0.2

[a]Confirmed to be *M. tuberculosis* by *hsp65* sequencing and morphology, [b]Confirmed by contracted RD16, [c]Confirmed by absence of RD2 and RD15, and contracted *SenX3-RegX3*, NT: Not tested.

Competing interests
The authors declare that they have no competing interests.

Authors' contributions
KC carried out the TLC assays, molecular genetic studies, sequence alignment and drafted the manuscript. AA, HY, TS, and TK cultured clinical isolates. HY helped to draft the manuscript. YK prepared reference strains. KT and HY collected clinical isolates. SM was responsible for planning the study. All authors read and approved the final manuscript.

Acknowledgements
We thank TAUNS Co, Ltd (Izunokuni, Japan) for providing the Capilia TB-Neo, SD MPT64, and TBc ID.

Author details
[1]Department of Mycobacterium Reference and Research, Research Institute of Tuberculosis, Japan Anti-Tuberculosis Association, Kiyose, Tokyo 204-8533, Japan. [2]Department of Basic Mycobacteriosis, Nagasaki University Graduate School of Biomedical Sciences, Nagasaki 852-8501, Japan. [3]Miroku Medical Laboratory Company Limited, 659-2 Innai, Saku, Nagano 384-2201, Japan.

Received: 21 August 2013 Accepted: 27 January 2014
Published: 1 February 2014

References

1. Public Health Mycobacteriology: **A guide for the level III laboratory.** In *Identification Test Techniques: Department of Health and Human Services.* Atran: Public Health Service. CDC; 1985.
2. Rastogi N, Goh KS, David HL: **Selective inhibition of the *Mycobacterium tuberculosis* complex by *p*-nitro-a-acetylamino-b-hydroxypropiophenone (NAP) and *p*-nitrobenzoic acid (PNB) used in 7H11 agar medium.** *Res Microbiol* 1989, **140**:419–423.
3. Goto M, Oka S, Okuzumi K, Kimura S, Shimada K: **Evaluation of acridinium ester-labeled DNA probes for identification of *Mycobacterium tuberculosis* and *Mycobacterium avium-Mycobacterium intracellulare* complex in culture.** *J Clin Microbiol* 1991, **29**:2473–2476.
4. Ioannidis P, Papaventsis D, Karabela S, Nikolaou S, Panagi M, Raftopoulou E, Konstantinidou E, Marinou I, Kanavaki S: **Cepheid GeneXpert MTB/RIF Assay for *Mycobacterium tuberculosis* detection and rifampin resistance identification in patients with substantial clinical indications of tuberculosis and smear-negative microscopy results.** *J Clin Microbiol* 2011, **49**:3068–3070.
5. Mitarai S, Okumura M, Toyota E, Yoshiyama T, Aono A, Sejimo A, Azuma Y, Sugahara K, Nagasawa T, Nagayama N, Yamane A, Yano R, Kokuto H, Morimoto K, Ueyama M, Kubota M, Yi R, Ogata H, Kudoh S, Mori T: **Evaluation of a simple loop-mediated isothermal amplification test kit for the diagnosis of tuberculosis.** *Int J Tuberc Lung Dis* 2011, **15**:1211–1217.
6. Richter E, Rüsch-Gerdes S, Hillemann D: **Evaluation of the genotype Mycobacterium assay for identification of Mycobacterial species from cultures.** *J Clin Microbiol* 2006, **44**:1769–1775.
7. Springer B, Stockman L, Teschner KD, Roberts G, Bottger EC: **Two-laboratory collaborative study on identification of Mycobacteria: molecular versus phenotypic methods.** *J Clin Microbiol* 1996, **34**:296–303.
8. Standardized Method for HPLC Identification of Mycobacteria: **Department of Health and Human Services.** Atranta: Public Health Service CDC; 1996.
9. Abe C, Hirano K, Tomiyama T: **Simple and rapid identification of *Mycobacterium tuberculosis* complex by immunochromatographic assay using anti-MPB64 monoclonal antibodies.** *J Clin Microbiol* 1999, **37**:3693–3697.
10. Hillemann D, Rüsch-Gerdes S, Richter E: **Application of the Capilia TB assay for culture confirmation of *Mycobacterium tuberculosis* complex isolates.** *Int J Tuberc Lung Dis* 2005, **9**:1409–1411.
11. Muyoyeta M, de Haas PE, Mueller DH, van Helden PD, Mwenge L, Schaap A, Kruger C, Gey van Pittius NC, Lawrence K, Beyers N, Godfrey-Faussett P, Ayles H: **Evaluation of the Capilia TB assay for culture confirmation of Mycobacterium tuberculosis infections in Zambia and South Africa.** *J Clin Microbiol* 2010, **48**:3773–3775.
12. Kodama A, Saito H: **Evaluation of CapiliaTB for identification of *Mycobacterium tuberculosis* complex, with special reference to the culture medium.** *Jpn Society Clin Microbiol (in Japanese)* 2007, **17**:109–118.
13. Hirano K, Aono A, Takahashi M, Abe C: **Mutations including IS*6110* insertion in the gene encoding the MPB64 protein of Capilia TB negative *Mycobacterium tuberculosis* isolates.** *J Clin Microbiol* 2004, **42**:390–392.
14. Nakajima C, Rahim Z, Fukushima Y, Sugawara I, Van der Zanden AGM, Tamaru A, Suzuki Y: **Identification of *Mycobacterium tuberculosis* clinical isolates in Bangladesh by a species distinguishable multiplex PCR.** *BMC Infect Dis* 2010, **10**:118.
15. Huard RC, Fabre M, de Haas P, Lazzarini LC, van Soolingen D, Cousins D, Ho JL: **Novel genetic polymorphisms that further delineate the phylogeny of the *Mycobacterium tuberculosis* complex.** *J Bacteriology* 2006, **188**:4271–4287.
16. Bedwell J, Kario SK, Behr MA, Bygraves JA: **Identification of substrains of BCG vaccine using multiplex PCR.** *Vaccine* 2001, **19**:2146–2151.
17. Seki M, Sato A, Honda I, Yamazaki T, Yano I, Koyama A, Toida I: **Modified multiplex PCR for identification of Bacillus Calmette-Guerin substrain Tokyo among clinical isolates.** *Vaccine* 2005, **23**:3099–3102.
18. Tuberculosis Research Committee (Ryoken): **Drug-resistant *Mycobacterium tuberculosis* in Japan: a nationwide survey, 2002.** *Int J Tuberc Lung Dis* 2007, **11**:1129–1135.
19. Morokuma Y, Uchida Y, Karashima T, Fujise M, Imamura S, Kayamori Y, Kang DC: **Identification of Mycobacterium tuberculosis Complex Strains in Kyushu University Hospital.** *J J Clin Microbiol (in Japanese)* 2008, **18**:177–182.
20. Muyoyeta M, Mwanza WC, Kasese N, Cheeba-Lengwe M, Moyo M, Kaluba-Milimo D, Ayles H: **Sensitivity, specificity, and reproducibility of the Capilia TB-Neo assay.** *J Clin Microbiol* 2013, **51**:4237–4239.
21. Yu MC, Chen HY, Wu MH, Huang WL, Kuo YM, Yu FL, Jou R: **Evaluation of the rapid MGIT TBc identification test for culture confirmation of *Mycobacterium tuberculosis* complex strain detection.** *J Clin Microbiol* 2011, **49**:802–807.
22. Sassetti CM, Boyd DH, Rubin EJ: **Genes required for mycobacterial growth defined by high density mutagenesis.** *Mol Microbiol* 2003, **48**:77–84.

doi:10.1186/1471-2334-14-54
Cite this article as: Chikamatsu *et al.*: Comparative evaluation of three immunochromatographic identification tests for culture confirmation of *Mycobacterium tuberculosis* complex. *BMC Infectious Diseases* 2014 **14**:54.

PLOS | ONE

RESEARCH ARTICLE

Structome Analysis of Virulent *Mycobacterium tuberculosis*, Which Survives with Only 700 Ribosomes per 0.1 fl of Cytoplasm

Hiroyuki Yamada[1]*, Masashi Yamaguchi[2], Kinuyo Chikamatsu[1], Akio Aono[1], Satoshi Mitarai[1]

1 Department of Mycobacterium Reference and Research, the Research Institute of Tuberculosis, Japan Anti-Tuberculosis Association, Kiyose, Tokyo, Japan, **2** Medical Mycology Research Center, Chiba University, Chiba, Japan

* hyamada@jata.or.jp

Citation: Yamada H, Yamaguchi M, Chikamatsu K, Aono A, Mitarai S (2015) Structome Analysis of Virulent *Mycobacterium tuberculosis*, Which Survives with Only 700 Ribosomes per 0.1 fl of Cytoplasm. PLoS ONE 10(1): e0117109. doi:10.1371/journal.pone.0117109

Academic Editor: Silvana Allodi, Federal University of Rio de Janeiro, BRAZIL

Received: October 14, 2014

Accepted: December 19, 2014

Published: January 28, 2015

Data Availability Statement: All relevant data are within the paper and its Supporting Information files.

Funding: This work was supported by a Health Science Research grant (H24-SHINKO-IPPAN- 011) from the Ministry of Health, Labour and Welfare of Japan. The funders had no role in study design, data collection and analysis, decision to publish, or preparation of the manuscript.

Competing Interests: The authors have declared that no competing interests exist.

Abstract

We previously reported the exquisite preservation of the ultrastructures of virulent *Mycobacterium tuberculosis* cells processed through cryofixation and rapid freeze substitution. Here, we report the "structome" analysis (i.e., the quantitative three-dimensional structural analysis of a whole cell at the electron microscopic level) of virulent *M. tuberculosis* using serial ultrathin sections prepared after cryofixation and rapid freeze substitution and analyzed by transmission electron microscopy. Five *M. tuberculosis* cells, which were contained in the serial ultrathin cross sections encompassing from one end to the other, were cut into 24, 36, 69, 55, and 63 serial ultrathin sections, respectively. On average, the cells were 2.71 ± 1.05 μm in length, and the average diameter of the cell was 0.345 ± 0.029 μm. The outer membrane and plasma membrane surface areas were 3.04 ± 1.33 μm^2 and 2.67 ± 1.19 μm^2, respectively. The cell, outer membrane, periplasm, plasma membrane, and cytoplasm volumes were 0.293 ± 0.113 fl (= μm^3), 0.006 ± 0.003 fl, 0.060 ± 0.021 fl, 0.019 ± 0.008 fl, and 0.210 ± 0.091 fl, respectively. The average total ribosome number was 1,672 ± 568, and the ribosome density was 716.5 ± 171.4/0.1 fl. This is the first report of a structome analysis of *M. tuberculosis* cells prepared as serial ultrathin sections following cryofixation and rapid freeze substitution and examined by transmission electron microscopy. These data are based on the direct measurement and enumeration of exquisitely preserved single-cell structures in transmission electron microscopy images rather than calculations or assumptions from indirect biochemical or molecular biological data. In addition, these data may explain the slow growth of *M. tuberculosis* and enhance understanding of the structural properties related to the expression of antigenicity, acid-fastness, and the mechanism of drug resistance, particularly in regard to the ratio of target to drug concentrations.

Introduction

Bacteria can be observed with the naked eye as turbidity in a liquid medium or as colonies on the surface of a solid medium. Under light or fluorescent microscopic analysis, bacteria appear as stained or fluorescence-emitting small round cocci or rod-shaped bacilli. These macroscopic and microscopic observations are equivalent to observing the biosphere from an aircraft flying at high altitude or observing large animals or tall plants on the earth's surface from an aircraft at low altitude. Although such observations provide surficial and numerical information useful for scientific and clinical investigations, they reveal only limited superficial information regarding individual bacterial cells. Biological phenomena occur in the cell envelope and cytoplasm of bacteria; therefore, we must utilize electron microscopy, particularly transmission electron microscopy (TEM), to observe the ultrastructure of bacteria in detail. Although TEM examinations of bacteria provide a variety of information, in general these examinations are highly qualitative because the intact cytoplasmic ultrastructure is poorly preserved by conventional chemical fixation, which makes it difficult to perform quantitative analyses.

Recent reports have revealed that cryofixation (CRF) and rapid freeze substitution (RFS) provide exquisite preservation of whole yeast and bacterial cells [1–8]. The authors of these studies examined various cellular properties and components using CRF-RFS–processed epoxy resin–embedded samples. Yamaguchi *et al.* determined the number and volume of organelles, including the mitochondria, endoplasmic reticulum, Golgi apparatus, and ribosomes using serial ultrathin sections of yeast cells. They proposed the term "structome" for this technique, which is defined as the 'quantitative and three-dimensional structural information of a whole cell at the electron microscopic level' [3, 5].

Mycobacterium tuberculosis, which is the causative agent of tuberculosis, contains a single, circular, double-stranded DNA molecule consisting of approximately 4.3 million base pairs, located in the cytoplasm [9]. Several investigators have calculated and estimated the number of mycobacterial cell components, including ribosomes, based on molecular biological and biochemical evidence [10–14].

Here, we report the results of a structome analysis of individual *M. tuberculosis* cells. *M. tuberculosis* cells were preserved by CRF-RFS and prepared for examination as serial ultrathin sections of epoxy resin–embedded cells. Cellular properties, including size, surface area, and volume, were directly measured based on electron micrographs, and the ribosomes scattered throughout the cytoplasm were enumerated. The ribosome density (number per 0.1 fl of cytoplasm) for *M. tuberculosis* was calculated and compared to that determined for yeast cells [2, 5] as well as previously published estimations [10–14]. This is the first report of a structome analysis of individual *M. tuberculosis* cells using serial ultrathin sections and direct enumeration. These data will aid future investigations of the fundamental cell biology, pathogenesis, and drug resistance of *M. tuberculosis*.

Materials and Methods

Bacteria

M. tuberculosis H37Rv (ATCC 27294) was cultured in 50 ml of Middlebrook 7H9 (Becton Dickinson, Sparks, MD, USA) supplemented with albumin (Fraction V), dextrose, and catalase enrichment (Becton Dickinson) and 0.05% Tween 80 contained in a 125-ml Erlenmeyer flask with a plain bottom (Nalgene, 4112–0125, NY, USA) for 2 weeks. Exponentially growing cells were used. Aliquots (1 ml) of cultured cells were transferred to sterile microcentrifuge tubes and centrifuged at 10,000 × *g* for 1 min. Usually, we used 6 ml of cultured cell suspension. The

supernatants were discarded, and the remaining pellets were collected in two microcentrifuge tubes.

CRF-RFS and epoxy resin embedding

The sandwich method was performed as described previously [2–7]. Briefly, a portion (<1 μl) of the highly concentrated bacterial pellet prepared as described above was applied to a glow-discharge-treated single-hole cupper grid (Veco; hole size, 0.1-mm diameter) and then sandwiched with another glow-discharge-treated single-hole grid. The grids were then picked up with tweezers and frozen by plunging them into melting propane (propane cooled with liquid nitrogen in a cooling device) for 20 seconds, as described previously [5]. The pair of grids was transferred, detached in liquid nitrogen, and immersed quickly into 2% osmium tetroxide/acetone solution and then placed in the device described above and cooled. Next, the samples were transferred from the bio-safety facility and placed in a freezer at −85°C for several days, after which they were allowed to come to room temperature over several days in a conventional area of the laboratory. Then, the osmium tetroxide/acetone solution was discarded and the samples were washed with absolute acetone three times at room temperature. The samples were then embedded in Spurr's resin using Leica/LKB Embedding Capsule Easy Molds (8-mm diameter) and polymerized at 70°C for 16 hours.

Preparation of serial ultrathin sections and TEM methods

More than 500 serial ultrathin sections with an average thickness of 55 nm were cut with an Ultracut E ultramicrotome (Reichert-Jung Co., Wien, Austria) equipped with a diamond knife and then picked up using single-slot cupper grids with a slot size of 2.0 × 1.0 mm (Maxtaform HF49, Tonbridge, UK) on 12 single-hole grids. Serial ultrathin sections were then transferred onto formvar support film mounted on an aluminum rack with 20 pores of 4-mm diameter [4]. The serial ultrathin sections were then dried, detached from the rack with support of the formvar, and stained with uranyl acetate and lead citrate. Of the 12 grids prepared, the serial ultrathin sections on 5 grids were damaged; therefore, the serial ultrathin sections on the remaining 7 grids were subjected to TEM examination. Among these 7 grids, serial ultrathin sections containing 5 cells on 5 grids were examined by TEM.

TEM examinations were performed using a JEOL JEM-1230 electron microscope operated at 80 kV. At the beginning of the examination, printed images of micrographs collected at low magnification (×2,000 to ×2,500) were searched for longitudinal cell profiles in the serial ultrathin sections in order to complete the examination at high magnification with a small number of serial ultrathin sections. However, because cell contents often dropped out from sections, especially those near the edge of the cell, serial cross sections encompassing the cell from one end to the other were searched at low magnification. Next, 5 cells in a total of 140 serial ultrathin sections were examined at higher magnification (×30,000, ×60,000, or ×80,000).

Image analysis and ribosome enumeration

Images obtained from negative scanning through Adobe Photoshop Elements (version 9) with CanoScan 8800F were saved as TIFF files and analyzed using ImageJ and Fiji software [15, 16]. Briefly, cell length was calculated by multiplying the number by 55 nm (representing the thickness of each section). The diameter (minor and major axes), perimeter, and thickness of the plasma membrane (PM), outer membrane (OM), and cell envelope of each cell were measured as a pixel value using the line selection menu in the ImageJ/Fiji window as well as a scale bar recorded on the same negative. Measured pixel values were converted to μm or nm according to the measured pixel value of the scale bar on the corresponding negatives.

The cross-sectional area of each cell was determined using the 'Measure' command in the 'Analyze' menu of ImageJ/Fiji by tracing the OM using the polygonal selection menu in the ImageJ window and converting the area result above into μm^2 by multiplying the square of the ratio of scale (nm) on the scanned negative by its pixel value. The cross-sectional area of each cell's cytoplasm was determined by tracing the PM in a like manner. The OM and PM surface areas (μm^2) were calculated as the cumulative area of a trapezium of the cell in each section using the formula for calculating the area of a trapezoid, where the perimeter of the OM and PM in a given section and the previous section were used as the upper base and lower base, respectively, and the section thickness (0.055 μm [55 nm]) was used as the height.

The volume (fl, = μm^3) of each cell was calculated as the cumulative volume of cylinders having the cell's cross-sectional area as the base and the section thickness (0.055 μm [55 nm]) as the height. The volumes of the OM and PM were calculated by multiplying the surface area of each membrane by its thickness (0.002 μm and 0.007 μm, respectively). The volume of the periplasm was calculated by subtracting the cytoplasmic and OM volumes from the cell volume.

Ribosomes as electron dense particles with 10 ~ 20 nm diameter in the cytoplasm of the cell cross-section in each serial ultrathin section were enumerated using the 'Multi-point Tool' in ImageJ/ Fiji [15, 16]. The total number of ribosomes in each cell and the number of ribosomes per 0.1 fl of cytoplasm were calculated based on the volume of each cell determined as described above.

Statistics

Averages and standard deviations for the diameter, area of the cross section in each serial ultrathin section, surface areas of the OM and PM, and cell volume were calculated for each cell and compared.

Results and Discussion

We previously reported the excellent preservation of the ultrastructure of *M. tuberculosis* cells provided by CRF-RFS [5, 7, 8]. CRF-RFS preserves not only the cell envelope with OM but also ribosomes within the cytoplasm.

In this study, more than 500 serial ultrathin sections were prepared from CRF-RFS samples, and five *M. tuberculosis* cells contained in the serial ultrathin sections were examined (Fig. 1, S1–S5 Figs.). Cell structures were measured and the number of ribosomes contained in the cytoplasm was determined. This is the first report of a structome analysis of individual *M. tuberculosis* cells, and there are no other reports describing the examination of bacteria in serial ultrathin sections prepared from epoxy resin–embedded CRF-RFS–preserved samples.

One-dimensional analysis

The length and diameter of five *M. tuberculosis* cells were measured using ImageJ/Fiji software, as described in the Materials and Methods section. Table 1 lists the results of a one-dimensional structome analysis of the five cells. Cells 1, 2, 3, 4, and 5 were cut into 24, 36, 69, 55, and 63 serial ultrathin sections, respectively. Cells 1, 2, 3, 4, and 5 were 1.32, 1.93, 3.80, 3.03, and 3.47 μm in length, respectively, for an average cell length of 2.71 ± 1.05 μm. As shown in S2 and S3 Figs., the serial ultrathin sections containing cells 2 and 3 were not continuous due to changing of the grid. That is, several serial ultrathin sections between numbers 30 and 31 for cell 2 and between numbers 67 and 68 for cell 3 may have been dropped out or mounted on the metal frame of the next grid (S2 and S3 Figs.). Therefore, these two cells may be slightly longer than the data. In addition, because cell length was determined based on the thickness of each serial ultrathin section and the number of serial ultrathin sections covering the cell, curved cells may

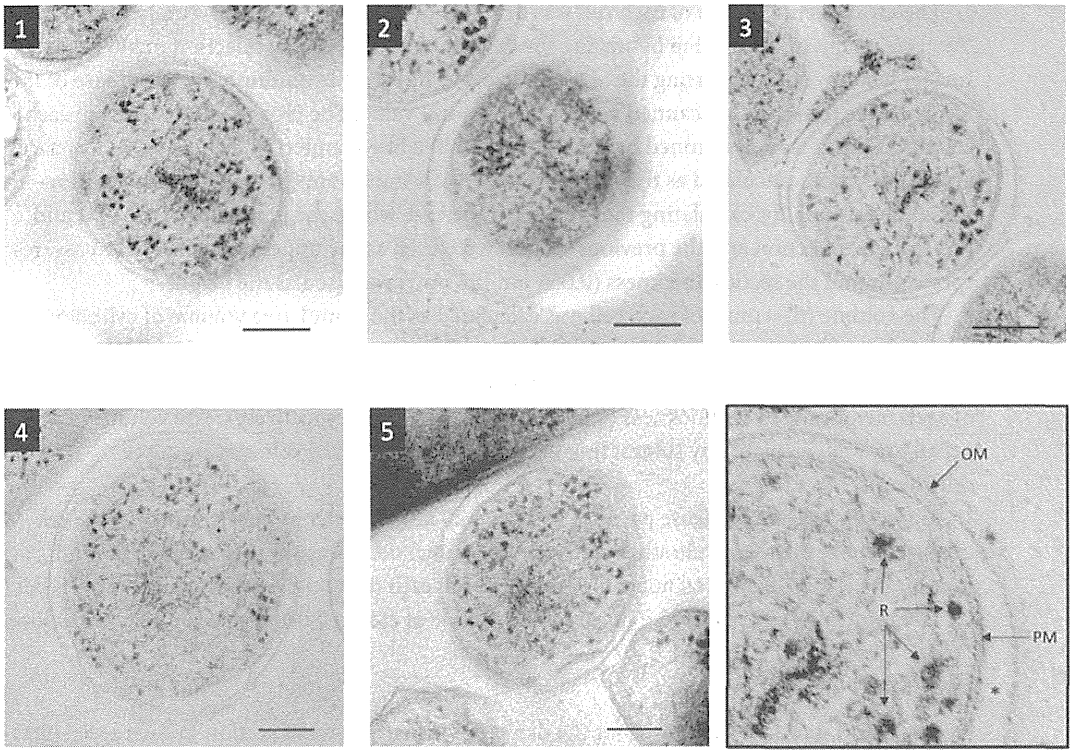

Figure 1. TEM images of five cross-sectioned *M. tuberculosis* cells. Cells were cut in the middle. The outer membrane (OM), periplasm (asterisk), plasma membrane (PM), and ribosomes (R) are visible as shown in the bottom right panel (enlarged image of cell 3). The cytoplasm of cell 2 appeared to have degraded, as evidenced by its dark color and fewer ribosomes. Cell 3 can be seen to the upper left of cell 2. Bar: 100 nm.

doi:10.1371/journal.pone.0117109.g001

be slightly longer than the calculated data indicate. Furthermore, because of examination protocol on serial ultrathin sections, whole cell profiles encompassing from one end to other can be observed in the shorter cells than the longer.

Cell diameter values were very similar, with average OM and PM diameters of 0.345 ± 0.029 μm (range, 0.293–0.366 μm) and 0.297 ± 0.022 μm (range, 0.273–0.326 μm), respectively. The average aspect ratio was 8.23 ± 3.60 (Table 1 and Fig. 2). Because the lengths of cells 3, 4, and 5 were 3-fold greater than that of the smallest cell (cell 1), it is suggested that cell division may occur independently of the length of the parent cell.

Table 1. One-dimensional profiles of *M. tuberculosis* cells.

Cell (Number of serial ultrathin sections) [1]	Length (μm)	Average Diameter (μm) (Cell)	Average Diameter (μm) (Cytoplasm)	Aspect Ratio
Cell 1 (24)	1.32	0.366	0.326	3.61
Cell 2 (35)	1.93	0.320	0.278	6.01
Cell 3 (69)	3.80	0.293	0.273	13.0
Cell 4 (55)	3.03	0.351	0.306	8.63
Cell 5 (67)	3.47	0.348	0.299	9.96
Average	2.71	0.345	0.297	8.23
SD	1.05	0.029	0.022	3.60

[1]Values in parenthesis indicate the number of serial ultrathin sections required to complete whole cell profile measurement.

doi:10.1371/journal.pone.0117109.t001

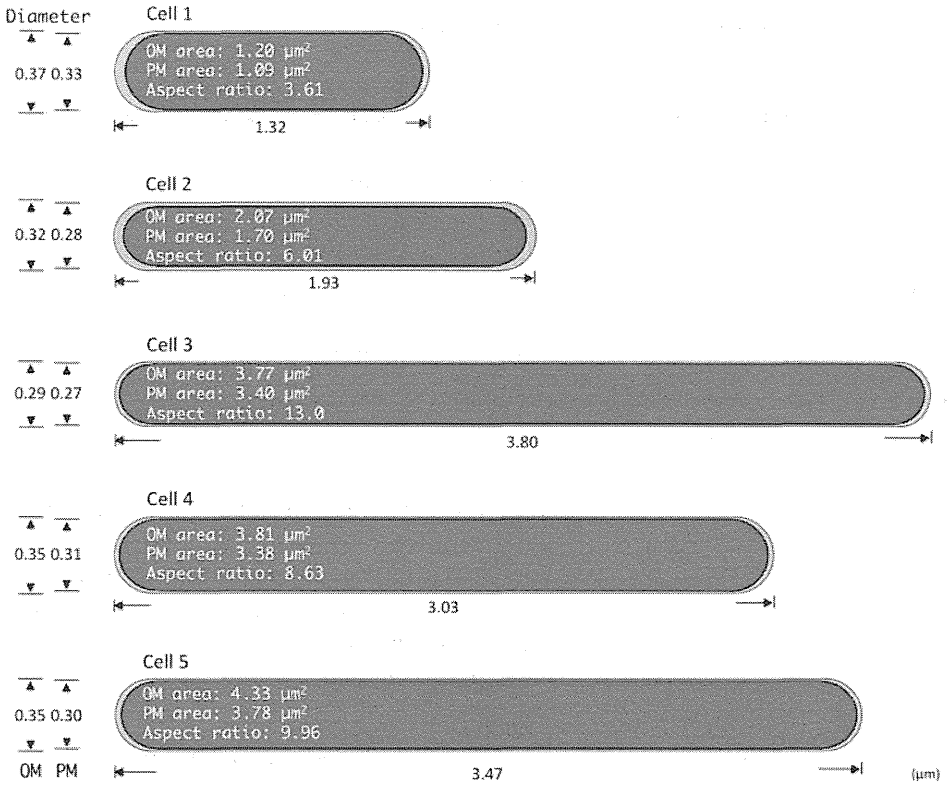

Figure 2. One- and two-dimensional properties of five *M. tuberculosis* cells obtained from serial ultrathin section TEM examination. The size of each schema correlates with the cell's relative width and length. The diameter, length, aspect ratio, outer membrane (OM) surface area, and plasma membrane (PM) surface area of each of five cells are indicated.

doi:10.1371/journal.pone.0117109.g002

Two-dimensional analysis

Two-dimensional profiles for the five *M. tuberculosis* cells were calculated from values measured using ImageJ/Fiji software, as described in the Materials and Methods section. Table 2 lists the average cross-sectional area of each whole cell (outlined by the OM), its cytoplasm (outlined by the PM), and the surface areas of the OM and PM. The average cross-sectional

Table 2. Two-dimensional profiles of *M. tuberculosis* cells.

Cell	Area (μm^2)			
(Number of serial ultrathin sections) [1]	Average Cross-section (Cell)	Average Cross-section (Cytoplasm)	Outer Membrane Surface	Plasma Membrane Surface
Cell 1 (24)	0.134	0.108	1.201	1.095
Cell 2 (35)	0.096	0.057	2.072	1.704
Cell 3 (69)	0.079	0.066	3.773	3.402
Cell 4 (55)	0.124	0.102	3.809	3.383
Cell 5 (67)	0.147	0.116	4.328	3.775
Average	0.116	0.090	3.037	2.672
SD	0.028	0.026	1.333	1.191

[1]Values in parenthesis indicate the number of serial ultrathin sections required to complete whole cell profile measurement.

doi:10.1371/journal.pone.0117109.t002

Table 3. Three-dimensional profiles of *M. tuberculosis* cells.

Cell	Volume (fl)				
(Number of serial ultrathin sections) [1]	Cell	Outer Membrane	Periplasm	Plasma Membrane	Cytoplasm
Cell 1 (24)	0.177	0.002	0.031	0.008	0.135
Cell 2 (35)	0.185	0.004	0.075	0.012	0.110
Cell 3 (69)	0.300	0.008	0.050	0.024	0.218
Cell 4 (55)	0.376	0.008	0.062	0.024	0.284
Cell 5 (67)	0.429	0.009	0.088	0.027	0.306
Average	0.293	0.006	0.060	0.019	0.210
SD	0.113	0.003	0.021	0.008	0.091

[1]Values in parenthesis indicate the number of serial ultrathin sections required to complete whole cell profile measurement.

doi:10.1371/journal.pone.0117109.t003

and cytoplasmic areas were 0.116 ± 0.028 μm^2 (range, 0.079–0.147 μm^2) and 0.090 ± 0.026 μm^2 (range, 0.057–0.116 μm^2), respectively (Fig. 2), and the average OM and PM surface areas were 3.037 ± 1.333 μm^2 (range, 1.201–4.328 μm^2) and 2.672 ± 1.1911 μm^2 (range, 1.095–3.775 μm^2), respectively. Because the surface areas of cells 3, 4, and 5 were 3-fold greater than that of the smallest cell (cell 1), it is suggested that cell division may occur independently of the surface area of the parent cell.

Three-dimensional (3D) analysis

The volume of each of the five *M. tuberculosis* cells was calculated using measurements taken with ImageJ/Fiji software, as described in the Materials and Methods section. Data regarding the 3D profile of each cell are shown in Table 3 and Fig. 3. The average whole-cell (as outlined by the OM) and cytoplasmic (as outlined by the PM) volumes were 0.293 ± 0.113 fl (range, 0.177–0.429 fl) and 0.210 ± 0.091 fl (range, 0.110–0.306 fl), respectively. In addition, the average OM, PM, and periplasmic volumes were 0.006 ± 0.003 fl (range, 0.002–0.009 fl), 0.019 ± 0.008 fl (range, 0.008–0.027 fl), and 0.060 ± 0.021 fl (range, 0.031–0.088 fl), respectively. Because the volumes of cells 3, 4, and 5 were 2-fold greater than that of the smallest cell (cell 1), it is suggested that cell division may occur independently of the volume of the parent cell.

Ribosome enumeration

The number of ribosomes in the cytoplasm of each cell was also determined (Table 4 and Fig. 3). This is the first report of the direct whole-cell enumeration of bacterial ribosomes in the cytoplasm based on TEM examinations of serial ultrathin sections images, as there are no previously published reports describing examinations of serial ultrathin sections of bacteria preserved by CRF-RFS. The average total ribosome number, average number per section, and average number per 0.1 fl of cytoplasm for the five cells examined in this study were 1,347 ± 877 (range, 49–2,122), 26.0 ± 18.6 (range, 1.4–36), and 583.2 ± 333 (range, 43.3–971), respectively.

Cell 2 contained only 49 ribosomes in the entire cell (not just in a single section), whereas each of the other 4 cells contained more than 850 ribosomes, and 3 of these cells (cells 3, 4, and 5) contained more than 1,600 ribosomes each. Some of the serial ultrathin sections of the cytoplasm of cell 2 showed even or scanty profiles, whereas other serial ultrathin sections were more electron dense (S2 Fig.). These profiles suggest that cell 2 was dead before RFS treatment and that degradation of the ribosomes had begun. This decomposition of cell 2 may be thought

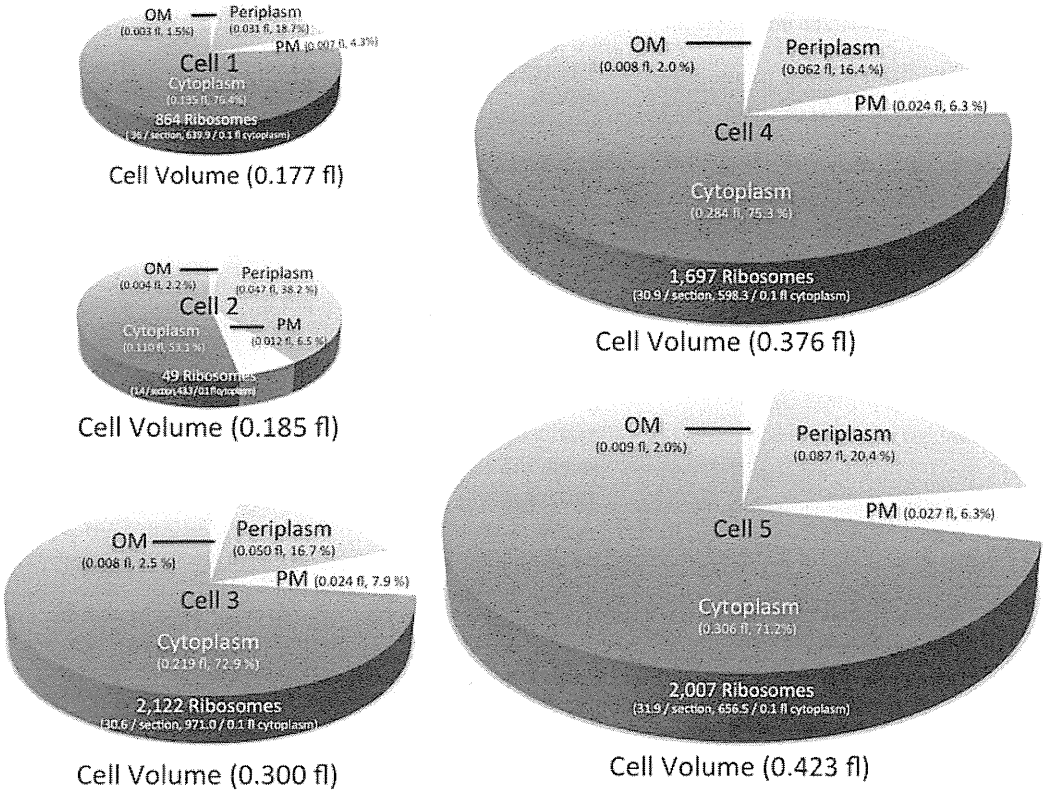

Figure 3. Pie graphs showing the volumes of the cell compartments for each of the five *M. tuberculosis* cells examined. The size of each pie correlates with the cell's relative volume. The whole-cell volume, proportion of the volumes of the cell compartments, total number of ribosomes, and ribosome density for each of five cells are indicated.

doi:10.1371/journal.pone.0117109.g003

of as an artifact of preparation resulting from CRF-RFS processing. However, it is highly unlikely that only cell 2 had begun to decompose due to processing because cells 2 and 3 coexisted in the same sections, as shown in Fig. 1, S2 and S3 Figs., and all cells, including cells 2 and 3, were prepared using the same procedure. In addition, the volume of the periplasmic space for cell 2 was relatively large (Table 3, Fig. 1 and S2 Fig.), a characteristic thought to be indicative of cytoplasm degradation. This suggests that cell 2 was already dead at the start of the CRF-RFS procedure. Excluding the data for cell 2, the average ribosome number per cell and the average ribosome number per 0.1 fl of cytoplasm for the remaining 4 cells were 1,672 and 716.5, respectively.

The number of ribosomes per *M. bovis* BCG cell has been estimated or calculated in several studies, with results ranging from 690 to 4,400 [10–13]. The calculated values were based on the proportion of rRNA in total RNA and the amount of ribosome-associated nucleotides [12]. Estimated numbers were based on the assumption that all of the transcribed rRNA molecules are used for the assembly of functional ribosomes with subunits of ribosome proteins, with no consideration given to rRNA molecules being derived from dead cells in the sample. In addition, because the ribosome numbers were estimated in bulk without measuring the volume of individual cells, the ribosome density could not be determined. Therefore, differences in ribosome enumerations based on estimates and direct observations suggest the possible presence of free rRNAs and free subunits of ribosomal proteins, which cannot be observed through TEM because these free molecules do not localize as high-electron-density particles. These

Table 4. Ribosome enumeration.

Cell (Number of serial ultrathin sections) [1]	Average per section (range)	Density per 0.1 fl	Total
Cell 1 (24)	36.0 (0–94)	640.2	864
Cell 2 (35)	1.4 (0–7)	43.3	49
Cell 3 (69)	29.8 (0–70)	971.0	2,122
Cell4 (55)	30.9 (0–89)	598.3	1,697
Cel5 (67)	31.9 (0–72)	656.5	2,007
Average	32.2 [26.0][2] (0–94)	716.5 [583.2][2]	1,672 [1,347][2]
SD	3.7 [18.6][2]	171.4 [333.0][2]	568 [877][2]

[1]Values in parenthesis indicate the number of serial ultrathin sections required to complete whole cell profile measurement.

[2]Values between square brackets are the calculation results including the value of cell 2.

doi:10.1371/journal.pone.0117109.t004

observations and interpretations indicate that determinations of rRNA copy number may lead to overestimation of the number of functional ribosomes and that precise enumeration of functional ribosomes requires direct observation of properly fixed and exquisitely preserved cytoplasm using TEM.

Comparison of ribosome density between *M. tuberculosis* and yeast

To date, there are only a few reports of quantitative structome analyses of microorganisms using TEM, including structome analyses of the yeast *Exophiala dermatitidis* and *Saccharomyces cerevisiae* [2, 6]. These studies reported values for the average number of ribosomes per 0.1 fl of 1,100 (11,000/fl) and 1,950 (19,500/fl) for *E. dermatitidis* and *S. cerevisiae*, respectively. In the present study, we found an average density of ribosomes in *M. tuberculosis* cells of approximately 720/0.1 fl, a density that is about one-half and one-third that of *E. dermatitidis* and *S. cerevisiae*, respectively (Table 5). The reported ribosome densities for *E. dermatitidis* and *S. cerevisiae* [2, 6] may be underestimates, as those studies enumerated ribosomes only in the cytoplasm and not in the nucleus, which comprises 7–10% of the cell volume. In addition, the study of *S. cerevisiae* compared structome data obtained in analyses of cells in both early G1 and late G1 phase. Other than a significantly higher number of autophagosomes in the cells in early G1 phase compared with late G1 phase, no other significant differences were observed, although the authors mentioned that the higher autophagosome number in early G1 phase cells may not be truly significant because the *P-value* was close to 5% [6]. These results suggest that there may be no significant differences in the ribosome density in *M. tuberculosis* cells between stationary and exponential phases, where it is difficult to determine whether a single *M. tuberculosis* cell within a population is in exponential phase or stationary phase, even with TEM.

Table 5. Comparison of ribosome number and density between *M. tuberculosis* and yeast cells.

Organism (Number of examined cell)	Density per 0.1 fl (range)	Average total ribosomes per cell (range)
M. tuberculosis (5)	716.5 [597.9][1]	1,672 [1,347][1]
	(640 ~ 971)	(864 ~ 2,122)
E. dermatitidis (5)[2]	1,100	195,000
	(970 ~ 1,340)	(112,000 ~ 336,000)
S. cerevisiae (6)[3]	1,950	195,000
	(1,770 ~ 2,060)	(115,000 ~ 272,000)

[1]Values between square brackets are the calculation results including the value of cell 2.

[2]Data described in reference 2.

[3]Data described in reference 6.

doi:10.1371/journal.pone.0117109.t005

Ribosome density–based drug targeting

With respect to ribosome-targeting drugs used in tuberculosis chemotherapy, few studies have examined the relationship between the number of target molecules in a single *M. tuberculosis* cell and the drug concentration in the environment surrounding the cell. For example, most cases of streptomycin (STR; $C_{21}H_{39}N_7O_{12}$; MW, 581.57 Da) resistance are attributed to mutations within either *rrs* in 16S rRNA, *rpsL* (encoding ribosomal protein S12), or *gidB* (encoding 7-methylguanosine [m^7G], a methyltransferase specific for rRNA) [17–19]. However, some STR-resistant strains harbor none of the above-mentioned mutations [20]. In this study, the average ribosome density was about 720 per 0.1 fl of cytoplasm, as calculated based on direct enumeration using serial ultrathin sections. In an environment containing STR at a concentration of 1.0 μg/ml (as is used in MGIT 960 drug susceptibility tests [21]), there would be about 100 STR molecules/0.1 fl. If the STR molecules could freely penetrate into the cytoplasm of *M. tuberculosis* cells and the concentration inside the cell is equal to that of the surrounding environment, the drug molecules will attack only one-seventh of ribosomes at any given point in time. It is not known how many direct binding events between ribosomes and STR molecules are required to kill a single bacterial cell. Therefore, because some cases of STR resistance cannot be explained by mutations in the target molecules, it is critical that the relationship between drug resistance and the drug to target molecule ratio be considered, along with how many drug molecules are required to kill a single bacterial cell and how many targets within a single bacterial cell must be attacked to effect killing.

Significance of structome analysis of serial ultrathin sections

In general, most microbiological studies are performed on clumps of bacterial cells or bulk bacterial populations, both of which may contain a large number of dead cells. The results of such studies are always expressed as average values, and these values may be under- or overestimations of the true values. In contrast, microscopy allows for direct observation of the dynamics of single cells with temporal or spatial continuity, enabling researchers to distinguish between living and dead cells. It is generally believed that because they share identical genetic information, all cells in a population of bacteria derived from a single strain should show the same phenotype, whether they are part of a colony or in suspension in liquid medium. However, it was recently reported that major differences in cell shape and susceptibility to antibiotics may exist between isogenic cells in a colony originating from a single cell [22–25]. Our structome

analyses show that the size properties and ribosome density may vary from cell to cell, even though the cells may be of the same strain. Time-lapse microscopy experiments and TEM structome analyses of serial ultrathin sections of single cells containing the same genomic information have revealed that individual cells have both similarities and differences, as is the case with human identical twins, whose fingerprints normally differ. This is the simplest demonstration that genes are not omnipotent [25]; that is, the final phenotype is not determined solely by genetic information. Therefore, we must observe living or properly fixed cells using suitable microscopy methods in order to understand the phenomena occurring in individual bacterial cells.

As mentioned in a previous report [6], 3D structural analyses are now possible thanks to newly developed techniques and devices, including electron tomography [26], cryo-electron microscopy with vitreous sections [26, 27], serial block-face–scanning electron microscopy [28], and focused ion beam–scanning electron microscopy [29]. These new techniques allow 3D reconstruction of protein molecules, microorganisms, organelles, and cells automatically in less time than conventional analyses using ultrathin sections and TEM. However, these techniques do have some drawbacks, including the possibility of blind angles in tomography, very low contrast in cryo-electron microscopy with vitreous sections, and degradation of cell components such as ribosomes as a result of treating specimens with reagents such as potassium ferric cyanide to enhance membrane contrast in focused ion beam–scanning electron microscopy and serial block-face scanning electron microscopy. Therefore, although these techniques have made 3D structural analyses easier to perform, the analyses themselves are exclusively qualitative rather than quantitative, and the resolution of the images obtained using these procedures is no better than that of conventional approaches involving TEM analysis of serial ultrathin sections. Nevertheless, future improvements in sample preparation and resolution in these new methods should overcome the above-mentioned problems and provide new approaches for structome analysis.

Conclusions

This is the first report of a TEM structome analysis of *M. tuberculosis* cells in serial ultrathin sections, based on direct measurement and enumeration of exquisitely preserved structures in living single cells rather than calculations or assumptions based on indirect biochemical or molecular biological data. Our data will enhance other investigations in fundamental biology, immunogenicity, and the pathogenicity of *M. tuberculosis*, as well as vaccine development, and mechanisms of drug resistance because our data about the surface area and the volume of PM and OM can provide insights into the capacity of these structures to contain various molecules, which may elicit immunogenicity and/or pathogenicity or may act as drug-target. In addition, our results will enhance quantitative analyses of drug-target interactions, particularly with respect to the drug to target molecule ratio of ribosome-targeting drugs.

Supporting Information

S1 Fig. Serial ultrathin section array of cell 1. A total of 24 serial ultrathin sections were cut to a thickness of 55 nm.
(TIF)

S2 Fig. Serial ultrathin section array of cell 2. A total of 36 serial ultrathin sections were cut to a thickness of 55 nm. Cell 3 is co-localized in the cross sections, as seen from top-left to bottom-left throughout the array. The cell profile ended at the 36th ultrathin section.
(TIFF)